

## Fischer–Tropsch Mechanism Revisited: Alternative Pathways for the Production of Higher Hydrocarbons from Synthesis Gas

Oliver R. Inderwildi,\* Stephen J. Jenkins, and David A. King

Department of Chemistry, University of Cambridge, Lensfield Road, Cambridge CB2 1EW, United Kingdom

Received: November 7, 2007; In Final Form: December 26, 2007

Evidence from density functional theory calculations that the main reaction pathway for the Fischer–Tropsch process on Co{0001} is not the carbide mechanism but an alternative branch starting with the hydrogenation of CO to an oxymethylidyne species. We show that hydrogenation is the main reaction path at realistic pressure using microkinetic simulations and thereby bridge the pressure gap in heterogeneous catalysis.

The Fischer–Tropsch process, in which higher hydrocarbons are manufactured from synthesis gas (CO/H<sub>2</sub> 2:1), is an important industrial process.<sup>1</sup> While in earlier times this process was mainly utilized to convert coal into liquid fuels (i.e., higher hydrocarbons), helping to circumvent oil embargos during WWII<sup>2</sup> and during the Apartheid regime in South Africa,<sup>1</sup> today it is once again of vital economic interest because it can also be utilized to convert biomass into liquid fuels.<sup>1</sup> It is thus a potential source of carbon-neutral fuels, which would help to mitigate global warming due to CO<sub>2</sub> emissions.<sup>3</sup>

Current opinion is that both CO and H<sub>2</sub> adsorb dissociatively on the catalytic metal surface and that both C and O are subsequently hydrogenated, yielding CH<sub>2</sub> and H<sub>2</sub>O. This is the carbide mechanism. While H<sub>2</sub>O desorbs, adsorbed CH<sub>2</sub> can undergo polymerization and hydrogenation reactions leading to alkane chains. Earlier, however, Storch et al. (see review by Schulz<sup>1</sup>) had suggested a mechanism in which a hydrogen adatom is added directly to the nondissociatively adsorbed CO molecule, leading to oxymethylidyne (CHO(s)) species (often referred to as formyl). This mechanism was once assumed to be the main reaction pathway, but such a view has fallen out of favor in more recent times, although Weinberg and co-workers detected such a species by bombarding CO on Ru{0001} with hydrogen radicals (i.e., via an Eley–Rideal mechanism)<sup>4</sup> and Rupprechter and co-workers were able to characterize such species spectroscopically during the dissociation of methanol on Pd{111}.<sup>5</sup> Watson et al., moreover, present indirect results from temperature program oxidation that CHO(s) is a plausible intermediate in the CH oxidation on Pt{110}.<sup>6</sup> We now revisit the possibility of a reaction pathway via such a species in the Fischer–Tropsch process on cobalt due to these recent results which strongly suggest that oxymethylidyne plays an important role in both the conversion of hydrocarbons<sup>6,7</sup> and carbonyl<sup>8–10</sup> surface species and also in the hydrogenation of CO<sub>2</sub> using a homogeneous catalyst.<sup>11,12</sup>

We studied the pathway of CO conversion to hydrocarbons on Co{0001} using state-of-the-art quantum-chemical density functional theory (DFT) slab calculations and microkinetic simulations. We present ample evidence that the carbide

**TABLE 1: Adsorption Energies on Co{0001}; All Values Are Given in eV per Atom/Molecule (in the Case of Hydrogen and Oxygen with Respect to H<sub>2</sub>(g) and O<sub>2</sub>(g))**

adsorbate	atop	hcp	fcc	bridged
CO	1.73	1.78	1.78	1.72
CO (with H <sub>(hcp)</sub> )		1.80	1.80	
H		0.51	0.48	
O		2.48	2.37	

mechanism is *not* the main reaction route on Co, and for the first time characterize the transition state for the surface hydrogenation of CO and the resulting CHO product. Moreover, we explain why this species is significantly more reactive than CO toward further reaction. Methodological details for the DFT calculations using CASTEP and the microkinetic simulations using DETCHEM can be found elsewhere.<sup>7,13</sup>

**Adsorption of CO, O, and H.** First, we examined the adsorption energies for CO, H, and O at high-symmetry sites, as summarized in Table 1, finding that each adsorbs preferentially in 3-fold hollow sites (hcp/fcc). Comparing the adsorption of CO with and without hydrogen as coadsorbate shows that there is a slight attractive lateral interaction between CO and H.

**Conversion of CO.** We also examined (I) the dissociation of CO from the hcp site and (II) the hydrogenation reaction from a starting position with CO and H coadsorbed in neighboring hcp positions (Figure 1, R). We find that the barrier to dissociation for CO on bare Co{0001} is 2.82 eV, which is considerably higher than the adsorption energy (1.8 eV). The adsorbed molecule desorbs rather than dissociates on this surface. These results agree with previous studies on the dissociation of CO on Co surfaces.<sup>14,15</sup> By contrast, hydrogenation leading to oxymethylidyne (Figure 1, P) requires a much smaller activation barrier of 1.31 eV.

Significantly, the CHO product is adsorbed with the oxygen atom bound to the surface: the cleavage of the C–O bond (i.e., CHO(s) → CH(s) + O(s)) is therefore facilitated, with a significantly lower barrier of 1.0 eV than for direct CO dissociation where the barrier is 2.8 eV. These results show that the hydrogenation route is the main reaction pathway on Co{0001}. Moreover, we find that the subsequent hydrogenation

\* E-mail: ori20@cam.ac.uk. Fax: +44 1223 33 65 36.

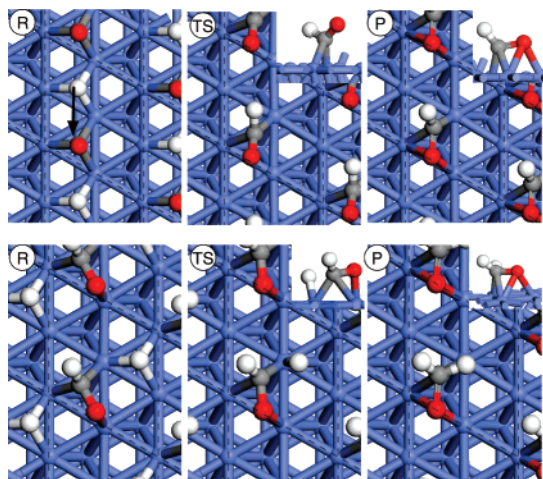


**Figure 1.** Reactant (R), transition state (TS), and product (P) of the hydrogenation of CO (top) and CHO (bottom) on Co{0001}; side views are shown as insets. Cobalt is shown as blue, oxygen as red, hydrogen as white, and carbon as gray.

of the CHO(s) species to CH<sub>2</sub>O(s) only requires an activation barrier of 0.45 eV and dissociation of the CH<sub>2</sub>O(s) species requires an activation barrier of 0.85 eV, while the dissociation of the CHO species requires 1.00 eV. (An obvious alternative reaction is the hydrogenation of the oxygen atom of the CHO(s) species leading to the surface alcohol species CHOH(s). This reaction, however, has an activation barrier of 0.81 eV and is therefore excluded in our microkinetic model. We have previously speculated that polarization of CO(s) by coadsorbed K promoter may enhance production of CHOH(s).<sup>24</sup>) Thus, hydrogenation of the CO species to CHO and CH<sub>2</sub>O successively weakens the C–O bond, which leads to lower activation barriers for its cleavage (CO, 2.82 eV; CHO, 1.00 eV; CH<sub>2</sub>O, 0.85 eV). An energy diagram of the different pathways is shown in Figure 2. Gong et al.<sup>16</sup> showed that the hydrogenation of CH(s) to CH<sub>2</sub>(s) has a lower barrier of 0.66 eV and is therefore a facile step. Nevertheless, since the barrier to CHO(s) hydrogenation to CH<sub>2</sub>O(s) is lower than the barrier to CHO(s) dissociation to CH(s), we eliminate this reaction pathway from our microkinetic model.

**Microkinetic Evaluation.** In order to evaluate the main pathway for synthesis of the monomer, we modeled the conversion of CO on Co{0001} microkinetically. Activation barriers and adsorption energies are taken from our DFT calculations; pre-exponential factors were estimated using the

transition state theory based on an assumed attempt frequency for unimolecular processes of 10<sup>13</sup> s<sup>-1</sup>, which has proven to be a viable assumption.<sup>17–19</sup> For a detailed discussion of the estimation of pre-exponential factors for surface reactions, we refer to ref 20. Sticking coefficients for hydrogen and CO were taken from the experimental literature.<sup>21,22</sup> (The detailed reaction mechanism can be found in the Supporting Information.) We neglect the hydrogenation of C(s), CH(s), and O(s) species. Therefore, CO conversion via the carbide mechanism would be characterized by formation of C(s), while reaction via CHO(s) decomposition would be characterized by formation of CH(s) in our microkinetic model. Hydrogenation via CHO(s) and CH<sub>2</sub>O(s) followed by decomposition would yield CH<sub>2</sub>(s). So long as C(s) and CH(s) intermediates are not formed in our model, we are safe in neglecting the carbide pathway.

We assume a starting coverage of 0.2 ML CO(s) and 0.4 ML H(s), with syn-gas in the ratio of 2:1 (H<sub>2</sub>/CO) at a pressure of 0.01 mbar above the surface. At low temperatures (<400 K), CO adsorbs on the surface and is the predominant surface species, with just a few percent of hydrogen coadsorbed (Figure 3, top). Above 400 K, conversion of CO is initiated: Both CHO(s) and CH<sub>2</sub>O(s) are present in a few percent of a monolayer and are hence true intermediates. Conversion of CO to CH<sub>2</sub>(s) continues until the surface is covered with 0.5 ML O(s) and 0.5 ML CH<sub>2</sub>(s), originating from the decomposition of CH<sub>2</sub>O(s) (Figure 3, top) (we note that polymerization reactions are not included in the model here). The calculation yields no formation of atomic carbon or CH(s), and hence, we eliminate the carbide mechanism. Carrying out the same calculation but excluding the hydrogenation steps, i.e., only adsorption, desorption, and dissociation, also confirms that CO would desorb before dissociating.

To take this microkinetic simulation to the next level, we studied the transient kinetics at 700 K and high pressure (30 bar). As can be seen from Figure 3 (bottom), initially CH<sub>2</sub>O(s) is formed but is rapidly depleted due to its conversion to CH<sub>2</sub>(s). Small amounts of CHO(s) are present on the surface throughout, but dissociation of this species (i.e., CH(s) formation) is not observed. Our model therefore clearly demonstrates that the main reaction pathway is the hydrogenation of CO, yielding CHO(s) and thence CH<sub>2</sub>O(s). It is the decomposition of this species to CH<sub>2</sub>(s) that gives rise to the building block for higher hydrocarbon formation.

It may be objected, of course, that dissociation reactions are much more likely at surface defects such as steps. Various studies show CO dissociation at steps, as found on corrugated

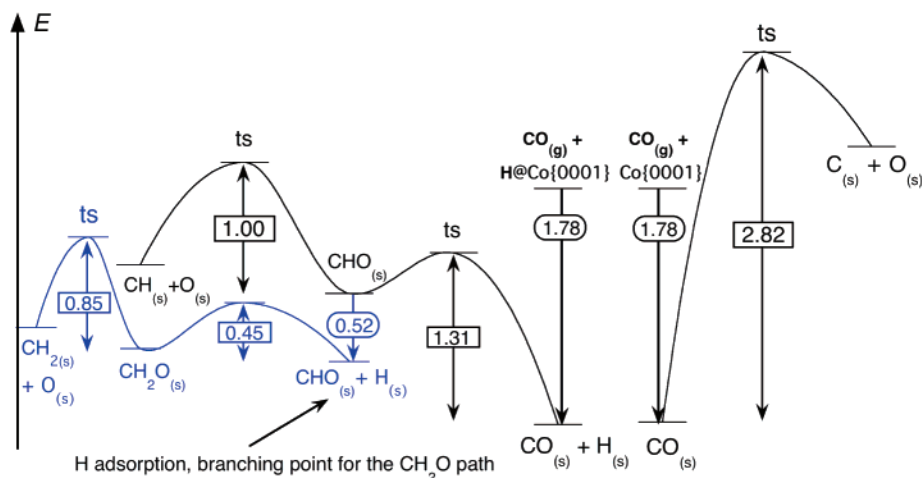


**Figure 2.** Energy diagram for CO dissociation and hydrogenation.

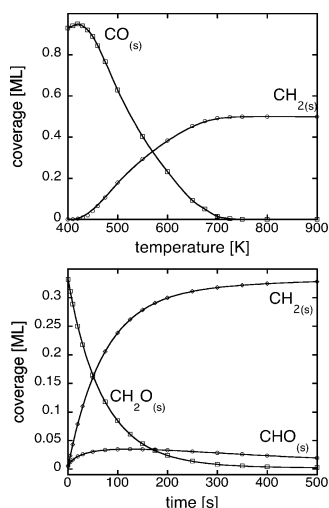


**Figure 3.** Equilibrated conversion of CO on Co{0001} as a function of temperature at 0.01 mbar (top) and the formation of CH<sub>2</sub>(s) as a function of time at 700 K and 30 bar (CO/H<sub>2</sub> 1:2) (bottom).

Co{0001} or on Co{10 $\bar{1}$ 2}.<sup>14,15</sup> Nevertheless, even *these* dissociation barriers are higher than the barriers found for hydrogenation and dissociation in our study. For example, Gong et al.<sup>15</sup> determined the dissociation barrier for CO at the steps of corrugated Co{0001} to be 1.61 eV, compared with our barrier of 1.31 eV for hydrogenation on the flat surface. Moreover, we have calculated the hydrogenation barrier for the corrugated surface studied by Gong et al.<sup>15</sup> to be 0.45 eV, which is lower again. This confirms our basic conclusion that CO(s) hydrogenation is the initiation step in the Fischer–Tropsch process when cobalt is the catalyst material.

**In Summary.** Adsorption followed by two hydrogenation steps successively weakens the triple bond of CO on cobalt to yield the CH<sub>2</sub>(s) building block for polymerization in the Fischer–Tropsch process. Moreover, after each hydrogenation step, the resulting species is adsorbed with its C–O bond parallel to the surface so that both oxygen and carbon are bound to the surface and activated for further hydrogenation and dissociation. Our work employs DFT calculations in combination with microkinetic simulations to bridge the pressure gap in heterogeneous catalysis and provide valuable insight into surface chemistry at high pressure. By these means, we calculate that the carbide mechanism is not viable on Co surfaces and that an alternative pathway via CHO(s) and CH<sub>2</sub>O(s) is preferred. It has to be noted, however, that this mechanism still needs experimental verification, which will unfortunately not be trivial, since the formyl species is (according to our calculation) an extremely short-lived species and only present at elevated pressure. Much excellent work has been done to bridge the

pressure gap;<sup>23</sup> it will, however, be difficult to spot short-lived species at realistic pressures. This rapid communication is therefore also meant to motivate experimentalists with an appropriate femtosecond spectroscopy apparatus to look out for such a species.

**Acknowledgment.** We acknowledge the EPSRC and DFG (O.R.I.) as well as The Royal Society (S.J.J.) for Research Fellowships. Dr. Herman Kuipers and colleagues at Shell Global Solutions are gratefully acknowledged for fruitful discussions.

**Supporting Information Available:** The elementary step reaction mechanism used for the kinetic simulation and the corresponding pre-exponential factors and activation barriers. This material is available free of charge via the Internet at <http://pubs.acs.org>.

## References and Notes

- Schulz, H. *Appl. Catal.*, A **1999**, 186, 3.
- Gordon, K.; et al. British Intelligence Objectives Sub-Committee Final Report No. 1697, Interrogation 667 Item No. 30. <http://www.fischer-tropsch.org>, 1946.
- King, D. A. *Science* **2004**, 303, 176.
- Mitchell, W. J.; Wang, Y. Q.; Xie, J.; Weinberg, W. H. *J. Am. Chem. Soc.* **1993**, 115, 4381.
- Borasio, M.; de la Fuente, O. R.; Rupprechter, G.; Freund, H. J. *J. Phys. Chem. B* **2005**, 109, 17791.
- Watson, D. T. P.; Harris, J. J. W.; King, D. A. *Surf. Sci.* **2002**, 505, 58.
- Inderwildi, O. R.; Jenkins, S. J.; King, D. A. *J. Am. Chem. Soc.* **2007**, 129, 1751.
- Mavrikakis, M.; Gokhale, A. A. *Abs. Pap. Am. Chem. Soc.* **2005**, 229, U861.
- Andersson, M. P.; Abild-Pedersen, F.; Remediakis, I.; Bligaard, T.; Jones, G.; Engbæk, J.; Lytken, O.; Horch, S.; Nielsen, J. H.; Sehested, J.; Rostrup-Nielsen, J. R.; Nørskov, J. K.; Chorkendorff, I. *J. Catal.*, in press.
- Huo, C. F.; Ren, J.; Li, Y. W.; Wang, J. G.; Jiao, H. J. *J. Catal.* **2007**, 249, 174.
- Urakawa, A.; Iannuzzi, M.; Hutter, J.; Baiker, A. *Chem.–Eur. J.* **2007**, 13, 6828.
- Urakawa, A.; Jutz, F.; Laurenczy, G.; Baiker, A. *Chem.–Eur. J.* **2007**, 13, 3886.
- Inderwildi, O. R.; Jenkins, S. J.; King, D. A. *Surf. Sci.* **2007**, 601, L103.
- Ge, Q. F.; Neurock, M. *J. Phys. Chem. B* **2006**, 110, 15368.
- Gong, X. Q.; Raval, R.; Hu, P. *Surf. Sci.* **2004**, 562, 247.
- Gong, X. Q.; Raval, R.; Hu, P. *J. Chem. Phys.* **2005**, 122.
- Wong, H. W.; Cesa, M. C.; Golab, J. T.; Brazdil, J. F.; Green, W. H. *Appl. Catal.*, A **2006**, 303, 177.
- West, R. H.; Celnik, M. S.; Inderwildi, O. R.; Kraft, M.; Beran, G. J. O.; Green, W. H. *Ind. Eng. Chem. Res.* **2007**, 46, 6147.
- Inderwildi, O. R.; Kraft, M. *ChemPhysChem* **2007**, 8, 444.
- Wang, Z.; Seebauer, E. G. *Appl. Surf. Sci.* **2001**, 181, 111.
- Ernst, K. H.; Schwarz, E.; Christmann, K. *J. Chem. Phys.* **1994**, 101, 5388.
- Klinke, D. J.; Broadbelt, L. J. *Chem. Eng. Sci.* **1999**, 54, 3379.
- Oosterbeek, H. *Phys. Chem. Chem. Phys.* **2007**, 9, 3570.
- Jenkins, S. J.; King, D. A. *J. Am. Chem. Soc.* **2000**, 122, 10610.